IOP PUBLISHING PHYSICS IN MEDICINE AND BIOLOGY

Phys. Med. Biol. **55** (2010) 6279–6297 doi:10.1088/0031-9155/55/20/015

Multifractal analysis of heart rate variability and laser Doppler flowmetry fluctuations: comparison of results from different numerical methods

Anne Humeau[1], Benjamin Buard[1,2], Guillaume Mahé[3], François Chapeau-Blondeau[1], David Rousseau[1] and Pierre Abraham[3]

[1] Laboratoire d'Ingénierie des Systèmes Automatisés (LISA), Université d'Angers, 62 avenue Notre Dame du Lac, 49000 Angers, France
[2] Groupe ESAIP, 18 rue du 8 mai 1945, BP 80022, 49180 Saint Barthélémy d'Anjou cedex, France
[3] Laboratoire de Physiologie et d'Explorations Vasculaires, UMR CNRS 6214-INSERM 771, Centre Hospitalier Universitaire d'Angers, 49033 Angers cedex 01, France

E-mail: anne.humeau@univ-angers.fr

Received 23 June 2010, in final form 2 September 2010
Published 5 October 2010
Online at stacks.iop.org/PMB/55/6279

Abstract

To contribute to the understanding of the complex dynamics in the cardiovascular system (CVS), the central CVS has previously been analyzed through multifractal analyses of heart rate variability (HRV) signals that were shown to bring useful contributions. Similar approaches for the peripheral CVS through the analysis of laser Doppler flowmetry (LDF) signals are comparatively very recent. In this direction, we propose here a study of the peripheral CVS through a multifractal analysis of LDF fluctuations, together with a comparison of the results with those obtained on HRV fluctuations simultaneously recorded. To perform these investigations concerning the biophysics of the CVS, first we have to address the problem of selecting a suitable methodology for multifractal analysis, allowing us to extract meaningful interpretations on biophysical signals. For this purpose, we test four existing methodologies of multifractal analysis. We also present a comparison of their applicability and interpretability when implemented on both simulated multifractal signals of reference and on experimental signals from the CVS. One essential outcome of the study is that the multifractal properties observed from both the LDF fluctuations (peripheral CVS) and the HRV fluctuations (central CVS) appear very close and similar over the studied range of scales relevant to physiology.

(Some figures in this article are in colour only in the electronic version)

1. Introduction

The cardiovascular system (CVS) incorporates complex biophysical processes with multiple levels of operation and regulation, and its complete understanding is still to be obtained. The most prominent processes involved in the CVS are heart beat dynamics and respiration. Other processes have also been identified such as myogenic, neurogenic and endothelial activities. All these processes together involve several characteristic time scales and their interplay. Multiscale analyses of biophysical data from the CVS can therefore be helpful in order to contribute to understanding the complex underlying dynamics.

The CVS can be studied through two viewpoints: a *central* viewpoint and a *peripheral* viewpoint. A central viewpoint is given by HRV signals. The latter are obtained from the time intervals between consecutive heart beats in the electrocardiogram (ECG). HRV therefore reveals information related to the heart itself and is thus of great interest for the diagnosis of cardiac pathologies. For a peripheral viewpoint of the CVS, the laser Doppler flowmetry (LDF) technique has been proposed in the 1970s. LDF relies on the interaction between the photons of a laser light—which is incident upon the tissues under study—and the moving blood cells of the microcirculation. The LDF signal, also called perfusion signal, comes from the first moment of the photocurrent power spectrum (see for example Rajan *et al* (2009), Humeau *et al* (2007), Shepherd and Öberg (1990) and Stern (1975)). New developments of the technique are also proposed (see for example Binzoni *et al* (2009), Wojtkiewicz *et al* (2009) and Liebert *et al* (2006)). This peripheral point of view allows for the diagnosis and follow-up of pathologies affecting the microvessels, among which we can find diabetes, peripheral arterial occlusive diseases and Raynaud's phenomenon (see for example Morales *et al* (2005), Humeau *et al* (2004) and Popivanov *et al* (1999)).

Through the analysis of HRV data, many multiscale and multifractal works have already been found useful in studying the central CVS (see for example Alam *et al* (2009), Baillie *et al* (2009), Sassi *et al* (2009), Ching and Tsang (2007), Guzman-Vargas *et al* (2005), Amaral *et al* (2001), Ivanov *et al* (2001), Havlin *et al* (1999), Ivanov *et al* (1999), Stanley *et al* (1999)). However, similar studies for the *peripheral* CVS are very recent (Humeau *et al* 2009) and need to be continued. Nevertheless, analyses from a peripheral viewpoint of the CVS lead to new requirements compared to analyses performed at the level of the central CVS. Thus, during the experiments with a laser Doppler flowmeter, the subject should not move at all, to avoid artifacts. As a result, only short LDF signals (a few minutes of data) can be recorded, whereas several hours of ECG data can be acquired through Holter systems.

The goal of this paper is to propose a study aimed at better understanding the CVS through a multiscale analysis of signal fluctuations. For this purpose, two steps are proposed: (1) a multifractal analysis of LDF fluctuations and (2) a comparison of this LDF analysis with the results obtained from HRV fluctuations recorded simultaneously with LDF signals. Comparisons of results obtained through data recorded simultaneously from the peripheral and central CVSs will therefore be possible. For these two steps, a suitable methodology to implement a multifractal analysis of LDF and HRV fluctuations needs to be identified.

Several methods have been proposed for the multifractal analysis of signals. Some of them are based on a box-counting technique which meshes the signal under study with various boxes of size ϵ and a normalized measure is computed in each box. The coarse-graining procedure implemented through such methods entails a natural and intuitive interpretation of the observations across scales. Two popular methods with the box-counting technique are the method from Halsey *et al* (1986), and the method proposed by Chhabra and Jensen (1989).

The multifractal properties of a signal can also be investigated through a structure function approach by calculating the qth-order structure function (Barabasi and Vicsek 1991). A time

increment existing in this method, and which is gradually increased for the analysis, also offers a natural and intuitive vision on the signal across scales.

Finally, other multifractal methods are based on the wavelet transform. The wavelet transform of a signal is used like an 'oscillating' box to represent its components. The most popular method from these ones is the wavelet-transform modulus-maxima (WTMM) method (Muzy *et al* 1993). In the latter, the local maxima of the modulus of the wavelet coefficients are extracted at each scale, in order to estimate the multifractal properties of the signal. Special care is sometimes required for its application on experimental signals, to avoid spurious maxima due to measurement noise.

Each of these methods contains different computation procedures that, even if they possess the same name, can lead to different quantities. Moreover, each method has its own parameters, and the values of the latter have to be chosen so that, when the methods are applied on synthetic signals, the results obtained are in accordance with the ones given by the theory.

In order to perform a targeted multifractal analysis of signals recorded from both the central and peripheral CVSs, we have to evaluate and compare several available methodologies, and especially their usefulness, applicability and interpretability for the biophysical problem that is addressed. The methods from Halsey *et al*, from Chhabra and Jensen, the method of the structure function, and the WTMM method are therefore first tested on synthetic signals.

In what follows, we first detail the multifractal methods tested. Afterwards, a comparison of their applicability and interpretability when implemented on simulated multifractal signals of reference is proposed. From the results, LDF and HRV fluctuations recorded simultaneously are processed. The multifractal spectra obtained for the peripheral and central CVSs are then analyzed, compared, and finally discussed.

2. Multifractal analysis methods

2.1. Method from Halsey et al

In the method from Halsey *et al*, the signal processed should be a normalized distribution (measure) (Halsey *et al* 1986). From this measure, the method allows the computation of a partition function $Z(q, \epsilon)$ from which the mass exponent function $\tau(q)$ and generalized fractal dimensions $D(q)$ are estimated. In order to apply the method from Halsey *et al*, first the signal has to be processed to obtain a non-negative measure $\{\gamma_i\}$. This can be performed by (1) pre-processing the signal to obtain non-negative data $\{s_i\}$; (2) dividing each sample of the resulting data $\{s_i\}$ by the sum of the samples for normalization to 1, i.e.

$$\gamma_i = \frac{s_i}{\sum_{i=1}^{N} s_i}, \tag{1}$$

where N is the number of samples in the non-negative signal $\{s_i\}$. LDF data are characterized by fluctuations superposed on a mean value. Because LDF signals are recorded in arbitrary units, and as the LDF signal mean value is probe-position-dependent, we suggest in what follows to focus on the signal fluctuations. Several studies have shown that these fluctuations contain physiological information (see for example Bernjak *et al* (2008), Kvandal *et al* (2006) and Stefanovska *et al* (1999)). The minimum value of each data is first subtracted from the data itself before computing the measure. Each sample of this positive signal is then divided by the sum of the signal samples, for normalization to 1 (step 2 mentioned above).

Each measure $\{\gamma_i\}$ is then processed to obtain the partition function $Z(q, \epsilon)$ as (Halsey *et al* 1986)

$$Z(q,\epsilon) = \sum_{i=1}^{N_{\text{boxes}}(\epsilon)} \mu_i^q(\epsilon), \tag{2}$$

where ϵ is the size (or scale) of the boxes used to cover the measure $\{\gamma_i\}$, $N_{\text{boxes}}(\epsilon)$ is the number of boxes of size ϵ needed to cover the measure $\{\gamma_i\}$, $\mu_i(\epsilon)$ corresponds to the sum of the sample values of the measure $\{\gamma_i\}$ on the ith box of size ϵ and the exponent q is a real parameter that indicates the order of the moment for $\mu_i(\epsilon)$. High values of the exponent q enhance boxes with relatively high values for $\mu_i(\epsilon)$, whereas low values of the exponent q favor boxes with relatively low values of $\mu_i(\epsilon)$.

If a log–log plot of the partition function $Z(q,\epsilon)$ versus ϵ shows straight lines, the partition function $Z(q,\epsilon)$ exhibits a power-law behavior. It therefore possesses a uniform and invariant behavior through the scales where the straight lines are present. On these scales, the mass exponent function $\tau(q)$ is estimated from the slope of the straight lines. The generalized fractal dimensions $D(q)$ ($q \neq 1$) are then estimated from $\tau(q)$ values as (Halsey *et al* 1986)

$$D(q) = \frac{1}{q-1}\tau(q). \tag{3}$$

For $q = 1$, the information dimension $D(1)$ is computed as the slope of

$$\sum_{i=1}^{N_{\text{boxes}}(\epsilon)} \mu_i(\epsilon)\log(\mu_i(\epsilon)) \tag{4}$$

versus $\log(\epsilon)$ on scales where (4) shows a power-law behavior. Finally, the Legendre transform of the mass exponent function $\tau(q)$ gives the multifractal spectrum $f(\alpha)$ as a function of the Hölder exponent α: $\alpha(q)$ is the derivative of $\tau(q)$ on the scales chosen for the power-law fitting and $f(\alpha)$ is computed as

$$f(\alpha(q)) = \alpha(q) \times q - \tau(q). \tag{5}$$

The Hölder exponent can be understood as a global indicator of the local differentiability for the processed measure.

2.2. *Chhabra and Jensen method*

The purpose of the Chhabra and Jensen methodology is to propose another box-counting procedure to evaluate the multifractal spectrum $f(\alpha)$, without resorting to the intermediate Legendre transform. In the Chhabra and Jensen method, a one-parameter normalized measure $\beta(q)$ is constructed where the probabilities in the boxes of size ϵ are (Chhabra and Jensen 1989; the meaning of $\mu_i(\epsilon)$ is the same as in the method from Halsey *et al* presented above)

$$\beta_i(q,\epsilon) = \frac{(\mu_i(\epsilon))^q}{\sum_j (\mu_j(\epsilon))^q}. \tag{6}$$

To determine the multifractal spectrum $f(\alpha)$, the slope of

$$\frac{\sum_i \beta_i(q,\epsilon)\log(\beta_i(q,\epsilon))}{\log(\epsilon)} \tag{7}$$

is first computed on the chosen scales ϵ. This gives $f(\alpha(q))$. Then, the slope of

$$\frac{\sum_i \beta_i(q,\epsilon)\log(\mu_i(\epsilon))}{\log(\epsilon)} \tag{8}$$

is computed on the same scales ϵ to give $\alpha(q)$. The multifractal spectrum $f(\alpha)$ is then obtained as a function of the Hölder exponent α.

2.3. Structure function method

In the structure function method, the qth-order structure function of the signal $\{s_i\}$ under study is defined as

$$C_q(l) = \frac{1}{N}\sum_{i=1}^{N} |s_i - s_{i+l}|^q, \tag{9}$$

where $N \gg 1$ is the number of samples over which the average is taken, and only terms with $|s_i - s_{i+l}| \neq 0$ are considered (Barabasi and Vicsek 1991). The mass exponents $\tau(q)$ are computed by linear least-squares fit to the double logarithm plot of $\log(C_q)$ versus $\log(l)$. By Legendre transforming the scaling exponents $\tau(q)$ of the structure function, one can obtain the multifractal spectrum $f(\alpha)$.

2.4. Wavelet transform modulus maxima method

In the WTMM method, the wavelet transform $T_\Psi[s]$ of the signal s under study is computed, and the sum of the qth powers of the local maxima of the wavelet transform coefficient modulus $|T_\Psi[s]|$ at scale ϵ defines the partition function $Z(q, \epsilon)$ (Muzy *et al* 1993):

$$Z(\epsilon, q) = \sum_{\alpha} |T_\Psi[s](x_\alpha(\epsilon), \epsilon)|^q, \tag{10}$$

where $\{x_\alpha(\epsilon)\}_\alpha$ is the set of coordinates supporting the maxima of the modulus for the wavelet transform. However, it is possible to get rid of some maxima with very low wavelet transform values (values which may lead to spurious divergences), by replacing (10) by (Muzy*et al* 1993)

$$Z(\epsilon, q) = \sum_{\alpha} (\sup_{x, \epsilon' \leqslant \epsilon} |T_\Psi[s](x_\alpha(\epsilon'), \epsilon')|)^q, \tag{11}$$

where $\sup_{x,\epsilon' \leqslant \epsilon}$ means that the supremum is taken for (x, ϵ') on each line of maxima at scales $\epsilon' \leqslant \epsilon$. Biophysical signals such as LDF and HRV data may give, in the wavelet transform, local maxima that correspond to low wavelet coefficients. The choice to take or not to take into account these low coefficients in the partition function computation can be a difficult task. Moreover, due to the not straightforward computation steps of the WTMM, the partition function $Z(q, \epsilon)$ obtained may be difficult to interpret. However, once the partition function $Z(q, \epsilon)$ is obtained, the mass exponents $\tau(q)$ and the multifractal spectrum $f(\alpha)$ can be computed as done in the method from Halsey *et al.*

In the WTMM method, the singularities are shifted by 1 with respect to the other methods, and thus the multifractal spectrum appears horizontally displaced by this value (Kestener and Arneodo 2003). In what follows, we have taken this shift into account when representing the results from the WTMM method, shifting WTMM multifractal spectra to obtain results that are directly comparable to those of the other methods.

2.5. Interpretation

From the above-mentioned equations, a signal is considered as multifractal if the corresponding measure has a nonlinear mass exponent function $\tau(q)$, or equivalently if it has nonconstant generalized dimensions $D(q)$ (Feder 1988). Therefore, the more multifractal a signal, the broader its multifractal spectrum. For a homogeneous fractal (monofractal data), the mass exponent function $\tau(q)$ is linear and the generalized dimensions $D(q)$ do not vary with the exponent q. The multifractal spectrum is therefore, in this case, a single point.

3. Application of the four multifractal analyses methods on synthetic signals

3.1. Synthetic signals

Herein the four multifractal methods (method from Halsey *et al*, method from Chhabra and Jensen, method of the structure function, and WTMM method) are first tested on binomial measures which are synthetic signals with known multifractal properties.

A binomial measure is recursively generated with a multiplicative cascade (Mandelbrot 1999). This cascade starts ($k = 0$) with a uniformly distributed unit of mass on the unit interval $I = I_0 = [0, 1]$. The next stage ($k = 1$) fragments this mass by distributing a fraction m_0 uniformly on the left half $I_{0.0} = \left[0, \frac{1}{2}\right]$ of the unit interval, and the remaining fraction $m_1 = 1 - m_0$ uniformly on the right half $I_{0.1} = \left[\frac{1}{2}, 1\right]$. At the next stage ($k = 2$) of the cascade, the subintervals $I_{0.0}$ and $I_{0.1}$ receive the same treatment as the original unit interval. At the kth stage of the cascade, the mass is fragmented over the dyadic intervals $[i2^{-k}, (i + 1)2^{-k}]$ where $i = 0, \ldots, 2^k - 1$ (Evertsz and Mandelbrot 1992). For binomial measures, the Hölder exponents α are defined as (Evertsz and Mandelbrot 1992)

$$\alpha = \frac{n_0}{k} v_0 + \frac{k - n_0}{k} v_1, \tag{12}$$

where n_0 is the number of digits 0 in the interval where the local exponent is computed, $v_0 = -\log_2(m_0)$ and $v_1 = -\log_2(m_1)$. Moreover, the multifractal spectrum $f(\alpha)$ is given by (Evertsz and Mandelbrot 1992)

$$f(\alpha) = -\frac{\alpha_{\max} - \alpha}{\alpha_{\max} - \alpha_{\min}} \log_2\left(\frac{\alpha_{\max} - \alpha}{\alpha_{\max} - \alpha_{\min}}\right) - \frac{\alpha - \alpha_{\min}}{\alpha_{\max} - \alpha_{\min}} \log_2\left(\frac{\alpha - \alpha_{\min}}{\alpha_{\max} - \alpha_{\min}}\right), \tag{13}$$

where $\alpha_{\min} = v_0$ and $\alpha_{\max} = v_1$.

In what follows, we apply the four multifractal methods on two binomial measures. The first binomial measure has $m_0 = 0.55$ and $m_1 = 0.45$, and is chosen because it presents a range of Hölder exponents similar to the range that will be met later on during the investigation of experimental LDF and HRV signals. The second binomial measure has $m_0 = 0.9$ and $m_1 = 0.1$ and therefore presents a larger multifractal spectrum. All these signals have 2^{14} samples and are shown in figure 1.

3.2. Choice of the parameters values

3.2.1. Parameter values for the Halsey et al method. In the method from Halsey *et al*, the measure is processed through three parameters: the scales or sizes ϵ of the boxes, the scales where the power-law fitting is performed (used for the estimation of the mass exponent function $\tau(q)$ and generalized fractal dimensions $D(q)$) and the values of q (exponent in the computation of the partition function $Z(q, \epsilon)$).

As mentioned above, the synthetic signals processed herein possess 2^{14} samples. Therefore, and in order to cover the whole signals, we choose all the powers of 2 for the sizes ϵ of the boxes.

In order to estimate the mass exponent function $\tau(q)$ and generalized fractal dimensions $D(q)$, the logarithm of the partition function $Z(q, \epsilon)$ has to be plotted versus the logarithm of the scales ϵ. On the scales where the partition function presents a power-law behavior (straight lines in the log–log plot), a power-law fitting can be performed. The slope of the latter is then used to compute the mass exponent function $\tau(q)$ and generalized fractal dimensions $D(q)$. We choose to perform the power-law fitting for the two synthetic signals on the whole range of scales, corresponding to 1 up to 2^{14} samples.

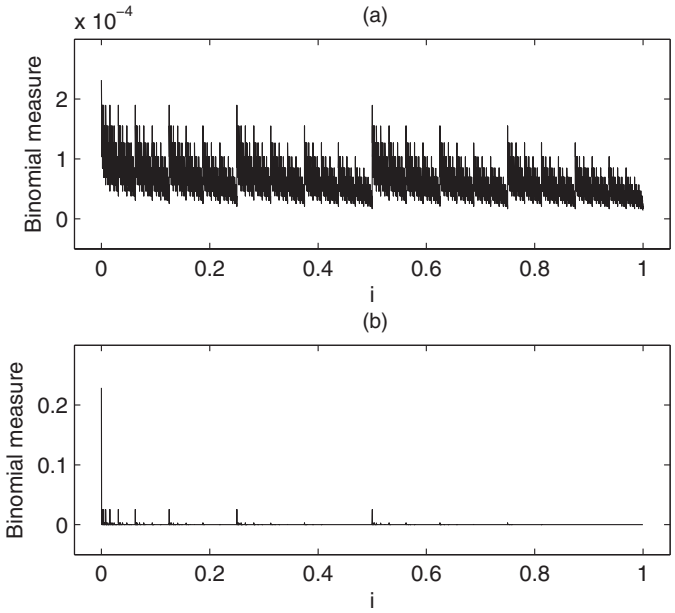

Figure 1. Binomial measures computed with (a) $k = 14$, $m_0 = 0.55$ and $m_1 = 0.45$; (b) $k = 14$, $m_0 = 0.9$ and $m_1 = 0.1$.

For the choice of the exponents q values, the lower the minimal negative value of the exponent q, the longer the right branch of the multifractal spectrum; the larger the maximal positive value of exponent q, the longer the left branch of the multifractal spectrum. Moreover, the higher the value of the exponent q, the more important the role played by possible outlier samples of high amplitudes in the values of the partition function $Z(q, \epsilon)$. As our synthetic signals do not have outlier samples, we choose to compute the moments on a rather large range of exponents q chosen so that the multifractal spectra $f(\alpha)$ obtained for the two binomial measures have branches that reach values near from 0 on their left and right parts. This choice is adopted in the method from Halsey *et al*, and from Chhabra and Jensen, in the structure function method, and in the WTMM method.

3.2.2. Parameters values for the Chhabra and Jensen method. In the Chhabra and Jensen method, the measure is processed with the same three parameters as for the method of Halsey *et al.* Thus, the sizes ϵ of the boxes, the scales for the power-law fitting (used for the estimation of the mass exponent function $\tau(q)$ and generalized fractal dimensions $D(q)$), and the values of q (exponent in the computation of the partition function $Z(q, \epsilon)$) have to be chosen. In order to compare the results given by the two box-counting methods for a given set of parameters, we choose—for the Chhabra and Jensen method—the same values as the ones of the Halsey *et al* method (for both the synthetic and physiological data).

3.2.3. Parameters values for the structure function method. With the structure function method, the signal under study has to be processed through an algorithm where three parameters have to be set: the values of the time increment l, the scales for the power-law fitting (used for the estimation of the mass exponent function $\tau(q)$) and the exponent q values. For the binomial measures, we choose all the possible powers of 2 from 1 for the time increment l values and choose the whole range of these values for the power-law fitting. Moreover,

as mentioned above, exponent q values are chosen so that the left and right branches of the multifractal spectra for the binomial measures reach values near from 0.

3.2.4. Parameters values for the WTMM method. When using the WTMM method, the following parameters have to be set:

- choice of the wavelet;
- the 'number' of local maxima used in the computation of the partition function $Z(q, \epsilon)$;
- the scales for the power-law fitting (used for the estimation of the mass exponent function $\tau(q)$ and generalized fractal dimensions $D(q)$) and
- the values of the exponent q.

The analyzing wavelet Ψ is generally chosen to be well localized in both space and frequency. Usually Ψ is only required to be of zero mean but for singularity tracking Ψ also has to be orthogonal to some low-order polynomials. A class of commonly used real-valued analyzing wavelets which satisfies these conditions is the successive derivative of the Gaussian function. In what follows, both $\Psi = -\theta'$ (where θ is the Gaussian function and $'$ means the derivative) and the Mexican hat wavelets are used.

The choice of the number of local maxima used in the computation of the partition function $Z(q, \epsilon)$ can be tricky; the applicability and interpretability of the WTMM method can accordingly become difficult. In what follows, this number is chosen so that the multifractal spectra obtained for the synthetic signals are the closest to the theoretical ones.

As it was set for the box-counting methods, the sizes ϵ of the boxes are chosen equal to all the powers of 2. Moreover, as for the box-counting methods, the power-law fitting is performed on scales corresponding to 1 up to 2^{14} samples, and the exponent q values are chosen so that the left and right branches of the multifractal spectra reach values near from 0.

As mentioned above, it is possible to get rid of some maxima with very low wavelet transform values by replacing the computation of $Z(q, \epsilon)$ mentioned in (10) by the one presented in (11) (Muzy *et al* 1993). These two algorithms will be tested thereafter. The Wavelab software was used for this purpose (http://www-stat.stanford.edu/∼wavelab/).

3.3. Results obtained for binomial measures

We applied the four multifractal methods on the binomial measures presented in figure 1. The results obtained with the method from Halsey *et al* are shown in figure 2. We can observe that the mass exponent functions $\tau(q)$, the generalized fractal dimensions $D(q)$ and the multifractal spectra $f(\alpha)$ are similar to the theoretical ones. This is true for the two binomial measures. The results obtained with the method from Chhabra and Jensen are also close to the theory, as shown in figure 3.

The multifractal spectra obtained with the structure function method are close to the theoretical results, as shown in figure 4. For the WTMM method we note (see figure 5) that the multifractal spectra obtained do not correspond to the theoretical values. This is true for the two binomial measures. Moreover, for the binomial measure that possesses a larger multifractal spectrum, the differences observed between the numerically estimated and the theoretical multifractal spectra are particularly predominant for the right part of the spectra (part which corresponds to the negative exponent q values). As noted by Turiel *et al* on other synthetic signals, the WTMM method generally provides a good description of the central part of the singularity spectrum, but in a very limited extent (Turiel *et al* 2006). Furthermore, as also found by Turiel *et al*, the WTMM method linearizes the right tail (Turiel *et al* 2006).

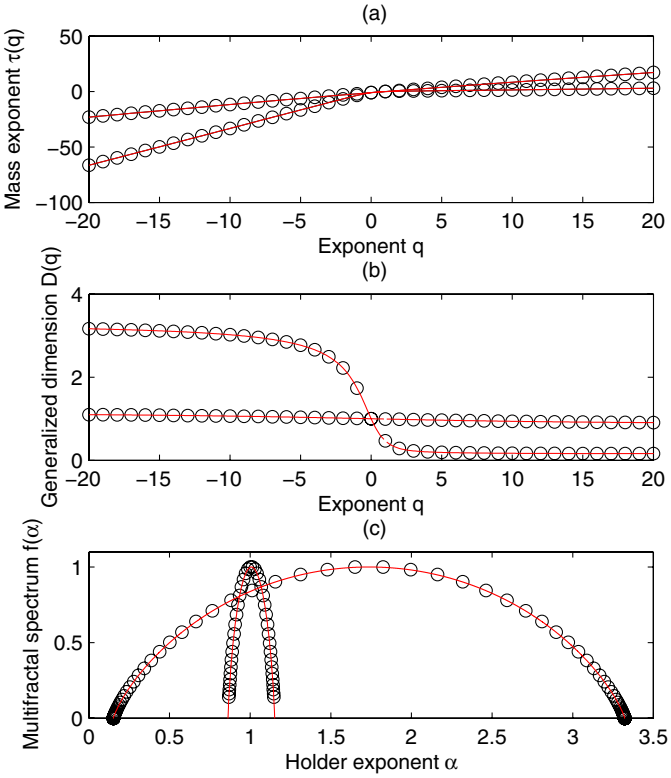

Figure 2. (a) Mass exponent functions $\tau(q)$, (b) generalized fractal dimensions $D(q)$ and (c) multifractal spectra $f(\alpha)$ obtained with the method from Halsey *et al* for the two binomial measures presented in figure 1. Solid line: theoretical values. Circles: numerically estimated values.

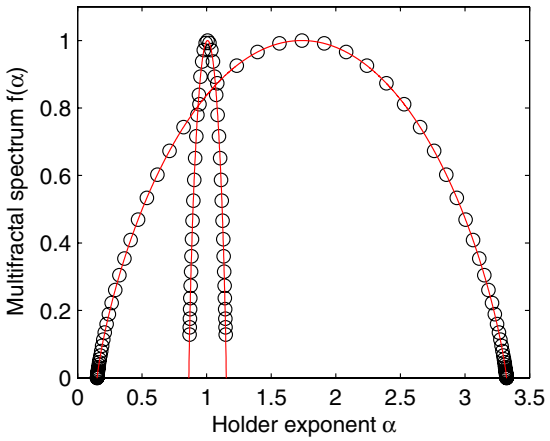

Figure 3. Multifractal spectra $f(\alpha)$ obtained with the method from Chhabra and Jensen for the two binomial measures presented in figure 1. Solid line: theoretical values. Circles: numerically estimated values.

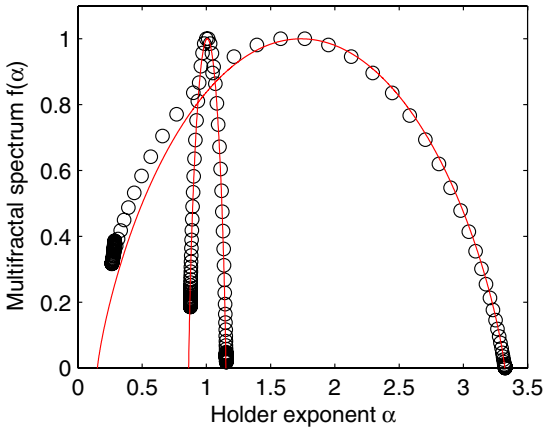

Figure 4. Multifractal spectra $f(\alpha)$ obtained with the structure function method for the two binomial measures presented in figure 1. Solid line: theoretical values. Circles: numerically estimated values.

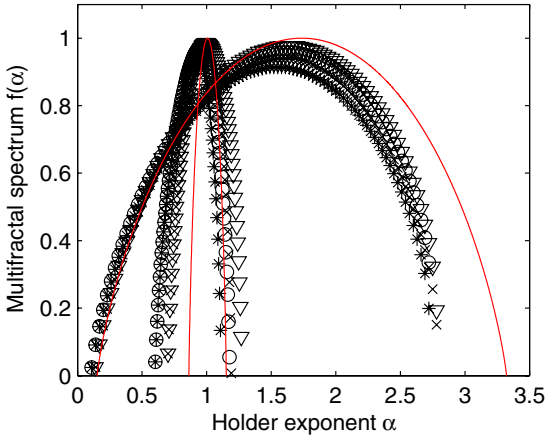

Figure 5. Multifractal spectra $f(\alpha)$ obtained with the WTMM method for the two binomial measures presented in figure 1. Solid line: theoretical values. $\circ$: numerically estimated results obtained with $\Psi = -\theta'$, where θ is the Gaussian function and (10) is chosen for the computation of the partition function $Z(q, \epsilon)$; *: numerically estimated results obtained with $\Psi = -\theta'$, where θ is the Gaussian function and (11) is chosen for the computation of the partition function $Z(q, \epsilon)$; $\triangledown$: numerically estimated results obtained with the Mexican hat for the wavelet and (10) is chosen for the computation of the partition function $Z(q, \epsilon)$; x: numerically estimated results obtained with the Mexican hat for the wavelet and (11) is chosen for the computation of the partition function $Z(q, \epsilon)$.

On the synthetic signals processed, the methods from Halsey *et al* and from Chhabra and Jensen give results that correspond to the theory. The principles and coarse-graining procedure used in these methods are easily interpretable. The structure function method gives results that are close to the theoretical ones. The method is, here again, quite intuitive. By contrast, the WTMM method gives results that do not fit the theory, and the choice of its parameters can be difficult. Its interpretability is also more difficult. Based on these results, we choose to apply hereafter the methods from Halsey *et al*, from Chhabra and Jensen, and the structure function method on LDF and HRV fluctuations.

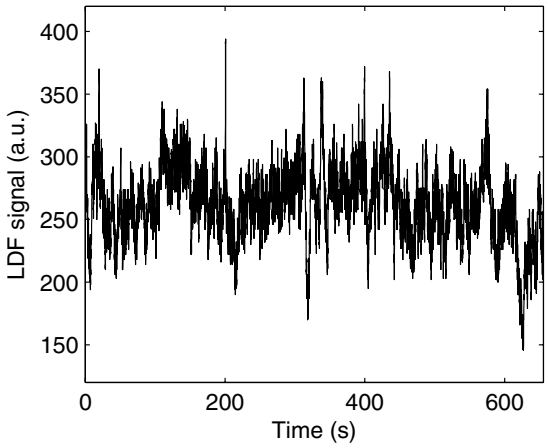

Figure 6. LDF signal recorded on the forearm of a healthy subject.

4. Application of three multifractal analyses methods on LDF and HRV fluctuations

4.1. Measurement procedure

For our study, LDF and ECG signals were recorded simultaneously, in 12 subjects (mean age 30.2 ± 11.5 years; 9 men, 3 women) without known disease. Each of them gave their written informed consent to participate before the beginning of the recordings. For the acquisition, the subjects were placed supine and left at rest for 15 min before each measurement. The temperature of the room was set at 23 ± 1 °C. For the LDF signal acquisition, a laser Doppler flowmeter (Periflux PF4001, Perimed, Stockholm, Sweden) and a laser Doppler probe (PF408, Perimed, Stockholm, Sweden) were used. The LDF probe was positioned on the forearm ventral face of the subjects. Skin blood flow was assessed in arbitrary units (au) and recorded on a computer via an analog-to-digital converter (Biopac System) with a sampling frequency of 250 Hz. A sub-sampling to 25 Hz was then performed. A Lifescope (Nihon Kohden Corporation) was used for the ECG acquisition for which the sampling frequency was chosen to be 1000 Hz. A sub-sampling to 250 Hz was then performed. LDF and ECG signals were recorded simultaneously for at least 20 min.

After acquisition, ECG signals were processed to obtain HRV signals. For this purpose, we developed a computer program to automatically detect the R peaks of the ECG time series. The results given by the automatic detection were visually checked and corrected if needed. The R–R intervals were then computed. Some of our LDF and HRV data are shown in figures 6 and 7, respectively.

Thereafter, 2^{14} samples of LDF signal fluctuations and 2^{10} samples of HRV data fluctuations are processed. This corresponds, respectively, to 10.9 min of LDF signals and to an average of 14.3 min of HRV data for our 12 subjects.

4.2. Choice of the parameters

4.2.1. Parameter values for the Halsey et al method. In what follows, the physiological data that are processed contain 2^{14} samples (LDF signals) and 2^{10} samples (HRV signals). For these signals, and as done for the synthetic signals, all the powers of 2 are chosen for the sizes ϵ of the boxes. Moreover, each signal is first processed to obtain a measure (see above).

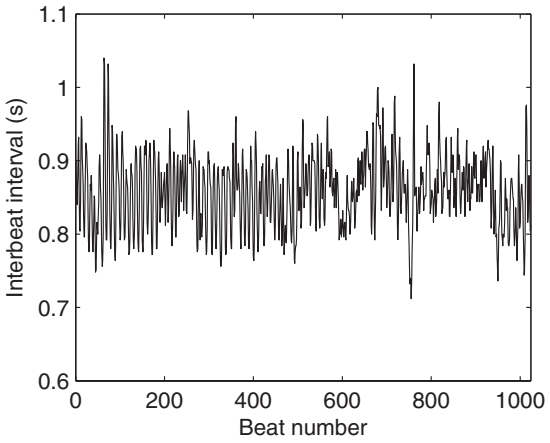

Figure 7. HRV signal recorded on a healthy subject.

For the estimation of the mass exponent functions $\tau(q)$ and generalized fractal dimensions $D(q)$, a log–log plot of the partition function $Z(q,\epsilon)$ versus ϵ has to be drawn. If the partition function $Z(q,\epsilon)$ presents a power-law behavior (straight lines in the log–log plot) a power-law fitting can be performed on the corresponding scales. We choose to perform the power-law fitting on scales in which significant physiological activities have been reported to occur. From the literature, LDF signals contain six physiological activities (see for example Bernjak *et al* (2008), Kvandal *et al* (2006) and Stefanovska *et al* (1999)): heart beats (time range [0.50 s, 1.66 s]), respiratory activity (time range [1.66 s, 6.89 s]), intrinsic myogenic activity (time range [6.89 s, 19.23 s]), neurogenic (sympathetic) activity (time range [19.23 s, 47.61 s]), nitric-oxide (NO)-dependent endothelial activity (time range [47.61 s, 105.26 s]) and non-NO-dependent endothelial activity (time range [105.26 s, 200 s]). Moreover, it has been shown that HRV signals also contain the respiratory, intrinsic myogenic, neurogenic, and NO-dependent endothelial activities (Bracic Lotric *et al* 2000). From all this, and in order to perform the linear fit on close scales for LDF and HRV fluctuations—to compare their mass exponent functions $\tau(q)$, generalized fractal dimensions $D(q)$, and multifractal spectra $f(\alpha)$—we choose to estimate the mass exponent functions $\tau(q)$ and generalized fractal dimensions $D(q)$ on scales between 10.24 s and 655.36 s for LDF fluctuations, corresponding to 2^8–2^{14} samples of LDF signals, and on scales between 8 s and 512 s for HRV fluctuations, corresponding to 2^3–2^9 samples of HRV data. These scales gather the intrinsic myogenic activity, the neurogenic activity, the NO-dependent endothelial activity and the non-NO-dependent endothelial activity.

Finally, because LDF and HRV fluctuations can possess outlier samples, the range of exponents q chosen for the computation of the partition function $Z(q,\epsilon)$ is reduced compared to the one chosen for the synthetic signals. We thereafter choose q between -3 and 3.

4.2.2. Parameter values for the Chhabra and Jensen method. As mentioned above, the same parameters as the ones chosen in the method of Halsey *et al* are taken into account for the method of Chhabra and Jensen. Moreover, each signal is first processed to obtain a measure (see above).

4.2.3. Parameter values for the structure function method. For the structure function method, we choose the time increment l and scale values for the power-law fitting that correspond

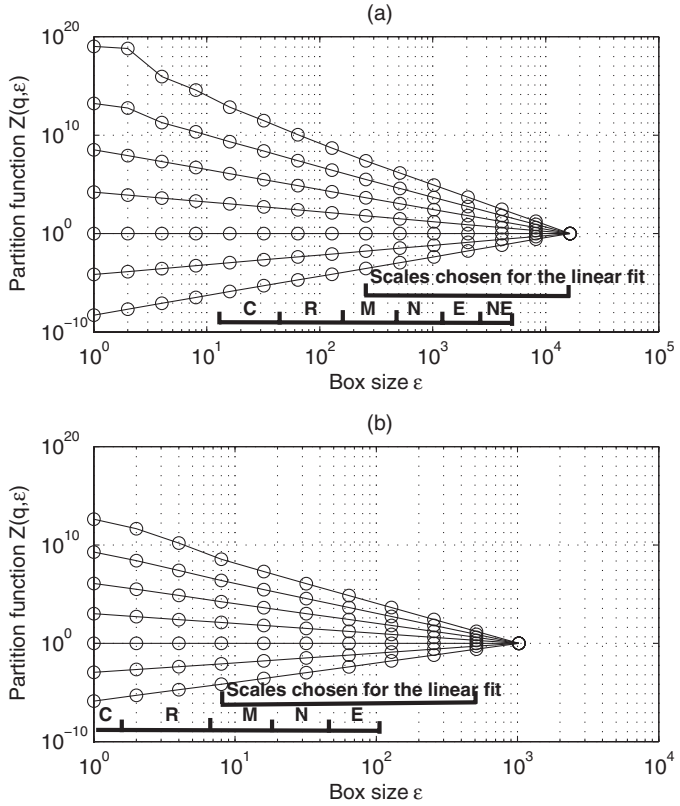

Figure 8. Partition function of (a) LDF and (b) HRV fluctuations recorded in a healthy subject obtained with the method from Halsey *et al.* The curves corresponding to q going from -3 to 3 by step of 1 are shown. The scales where the physiological activities take place are represented: C, R, M, N, E and NE stand, respectively, for cardiac activity, respiratory activity, myogenic activity, neurogenic activity, NO-dependent endothelial activity and non-NO-dependent endothelial activity.

(the most) to the values of the boxes and power-law fitting scales chosen in the box-counting methods. Thus, for LDF signals, the time increment l goes from 1 to 2^{13} (2^{14} cannot be used as it corresponds to the length of the signals) and the scales chosen for the power-law fitting are 2^8–2^{13} samples. In the same way, for HRV signals, we choose the time increment l from 1 to 2^9 and scales 2^3–2^9 for the power-law fitting. Furthermore, the q values are set from -3 to 3. Finally, as for the box-counting methods, each signal is first processed to obtain a measure (for comparisons).

4.3. Results and discussion

For the Halsey *et al* method and when exponent q goes from -3 to 3, the partition functions $Z(q, \epsilon)$ of all our LDF signals show a power-law behavior on scales going from 10.24 s to 655.36 s (scales corresponding to 2^8 up to 2^{14} samples of LDF signals; see figure 8(a)). Moreover, for all our HRV data and for the set of parameters chosen in the method from Halsey *et al*, the partition functions $Z(q, \epsilon)$ show a power-law behavior from 8 s to 512 s (scales corresponding to 2^3 up to 2^9 samples of HRV data); see an example in figure 8.

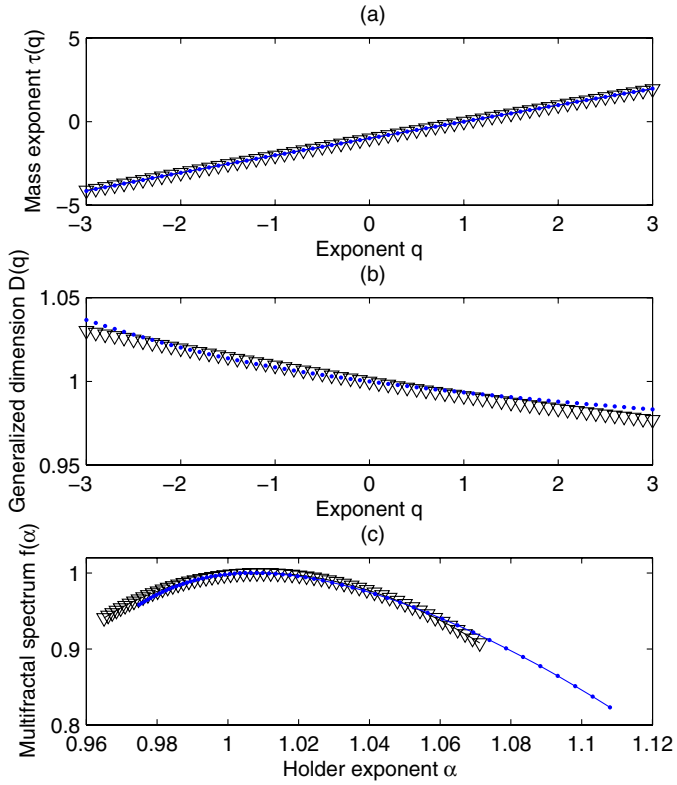

Figure 9. (a) Average mass exponents $\tau(q)$, (b) average generalized fractal dimensions $D(q)$ and (c) average multifractal spectra $f(\alpha)$ obtained with the method from Halsey *et al* for 12 LDF signals (curve with triangles) and for 12 HRV signals (dotted curve) recorded in 12 healthy subjects. The power-law fitting has been performed on scales going from 10.24 s to 655.36 s (scales corresponding to 2^8–2^{14} samples) for LDF fluctuations, and from 8 s to 512 s (scales corresponding to 2^3–2^9 samples) for HRV fluctuations.

All our partition functions $Z(q, \epsilon)$ computed with the method from Halsey *et al* therefore exhibit a power-law behavior, or a linear behavior in log–log coordinates, on the scales chosen for the linear fitting. Thus, for both LDF and HRV fluctuations, our results show a homogeneous power-law behavior over the range of scales where four distinct physiological activities have been reported by authors (see for example Bernjak *et al* (2008), Kvandal *et al* (2006), Stefanovska *et al* (1999), Bracic Lotric *et al* (2000)).

The average estimated mass exponent function $\tau(q)$ and generalized fractal dimensions $D(q)$ computed with the method from Halsey *et al* for the 12 subjects are shown in figures 9(a) and (b), respectively, for LDF and HRV fluctuations. From these figures we can note that the average estimated mass exponent functions $\tau(q)$ for both LDF and HRV fluctuations are very similar. The mass exponent functions $\tau(q)$ are close to the straight line $\tau(q) = q - 1$ which is the mass exponent function for a uniform measure. Moreover, the average generalized fractal dimensions $D(q)$ are also very close for LDF and HRV fluctuations. Thus, the average generalized fractal dimensions for LDF fluctuations are observed from 1.03 to 0.97 when exponent q varies between -3 and 3. For HRV fluctuations, the average generalized fractal dimensions D are observed from 1.03 to 0.98 when the exponent q goes from -3 to 3.

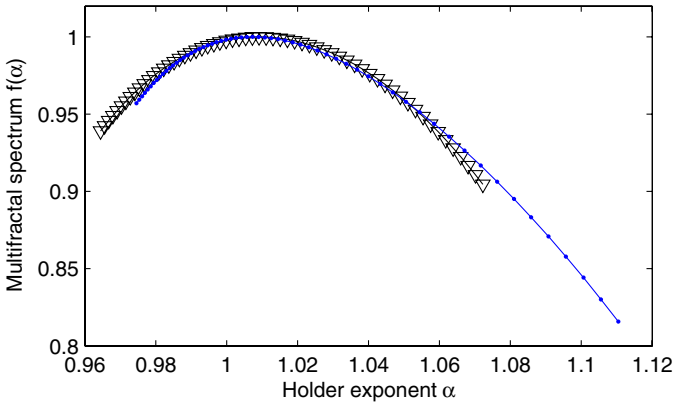

Figure 10. Average multifractal spectra $f(\alpha)$ obtained with the method from Chhabra and Jensen for 12 LDF signals (curve with triangles) and for 12 HRV signals (dotted curve) recorded in 12 healthy subjects. The power-law fitting has been performed on scales going from 10.24 s to 655.36 s (scales corresponding to 2^8–2^{14} samples) for LDF fluctuations, and from 8 s to 512 s (scales corresponding to 2^3–2^9 samples) for HRV fluctuations.

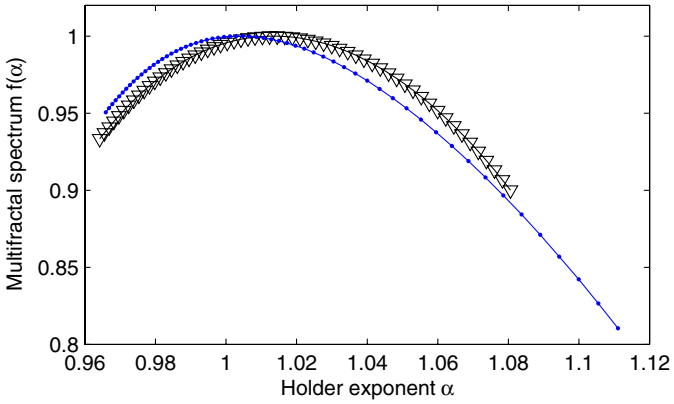

Figure 11. Average multifractal spectra $f(\alpha)$ obtained with the structure function method for 12 LDF signals (curve with triangles) and for 12 HRV signals (dotted curve) recorded in 12 healthy subjects.

The average estimated multifractal spectra obtained for LDF and HRV fluctuations with the method from Halsey *et al* are shown in figure 9(c). We can observe that the widths of these two estimated multifractal spectra are close and rather narrow.

For the Chhabra and Jensen method, the average estimated multifractal spectra obtained for LDF and HRV fluctuations are shown in figure 10. We can observe that these average multifractal spectra are very close for LDF and HRV fluctuations and close to the ones computed with the method from Halsey *et al* (see figure 9(c)).

The structure function method gives the average multifractal spectra shown in figure 11 for LDF and HRV fluctuations. We can observe that the multifractal spectra obtained for LDF and HRV fluctuations are nearly the same. Moreover, these multifractal spectra are only slightly different from the ones estimated with the two box-counting methods (methods from Halsey *et al* and from Chhabra and Jensen; see figures 9(c) and 10). Yordanova *et al* noted

that since the fractal functions may have, at any scale, increments close to zero, the structure function can diverge for $q < 0$ (Yordanova *et al* 2004). Furthermore, some authors mentioned that the structure function method cannot deal with the divergence problems inherent to the computation of negative-order exponents without losing the natural Legendre transform bridge with the multifractal spectrum (Muzy *et al* 1993). This could explain the small differences between the results of the structure function method and the two box-counting methods.

Some authors have shown that multifractality of HRV data from healthy subjects is observed at a higher value than the one observed in patients with congestive heart failure (Havlin *et al* 1999, Ivanov *et al* 1999). Moreover, such multifractality reported in HRV signals of healthy subjects has been found to be related to the intrinsic properties of the control mechanisms in human heartbeat dynamics and not simply due to changes in external stimulation and the degree of physical activity (Amaral *et al* 2001). Some authors hypothesized that both the monofractality and weaker anticorrelations for heart failure dynamics could be related, at least in part, to impaired parasympathetic control in congestive heart failure patients (Amaral *et al* 2001). Moreover, by computing the fractal dimension of heart rate and blood pressure in healthy and diabetic subjects, some authors found a lower fractal dimension of heart rate in diabetic patients than in healthy subjects but a similar fractal dimension of systolic blood pressure in the two groups (Chau *et al* 1993).

Compared to the other multifractal studies performed on the signals of the CVS, our work processes and compares the multifractal spectra of signals recorded simultaneously from the peripheral and the central CVSs. From our results and through three different multifractal methods, we show that LDF and HRV fluctuations possess similar narrow multifractal spectra, on the scales studied. All this could mean that the corresponding fluctuations may have close weak multifractal properties on the scales studied. Our work focuses on a multifractal analysis of LDF and HRV *signals*. Both kinds of signals correspond to different physiological meanings. HRV data are computed from the time intervals between consecutive heart beats in the ECG, whereas LDF signals are extracted from the first moment of a photocurrent power spectrum computed from backscattered photons of a laser light. Therefore, from our multifractal results, no physiological comparisons can be drawn; only signal multifractal properties are compared.

Using the method from Chhabra and Jensen for the estimation of the generalized fractal dimensions $D(q)$ and multifractal spectrum $f(\alpha)$ of HRV signals, other authors have shown that the variations of D with q and the width of the multifractal spectrum $f(\alpha)$ are low (see for example Guzman-Vargas *et al* (2005) and Munoz-Diosdado *et al* (2005), where around 8 h and 2 h of data are computed).

In the frame of a multifractal analysis with the methods from Halsey *et al*, from Chhabra and Jensen, or with the structure function method, some criteria could be suggested regarding the minimum length of recording and the choice of the sampling frequency for LDF signals: if one wants to perform the power-law fitting on scales in which significant physiological activities have been reported to occur, then the minimum length of recording should correspond to the longest period of the targeted activities. In our work, for LDF signals, we have chosen to perform the power-law fitting on scales gathering the intrinsic myogenic activity, neurogenic activity, NO-dependent endothelial activity and non-NO-dependent endothelial activity. The period of the latter activity is the longest of the four (time range [105.26 s, 200 s]). Therefore, at least 200 s of LDF signal was necessary. Regarding the sampling frequency of the signal, the highest its value, the smaller the time increment between two samples, and therefore the smaller—temporal precision—can be the sizes ϵ of the boxes (in the methods from Halsey *et al*, and Chhabra and Jensen) or of the time increment (in the structure function method).

The results obtained in the present study complement the previous multifractal analysis of data recorded simultaneously from the peripheral and central CVSs (Humeau *et al* 2009). Our work focuses here on the fluctuations of the LDF and HRV data; the influence of the mean value of each signal was removed by processing data where the minimum value of each signal was subtracted. This has not been performed in a previous work (Humeau *et al* 2009). As shown in many studies, the fluctuations of LDF and HRV signals contain physiological information (see for example Bernjak *et al* (2008), Kvandal *et al* (2006), Bracic Lotric *et al* (2000), Stefanovska *et al* (1999)). Furthermore, herein several numerical multifractal analysis methods are tested and compared. Moreover, the power-law fitting is performed on scales where physiological activities have been reported. The scales chosen for the power-law fitting in a previous work were different, as well as the choice of the q-values (Humeau *et al* 2009). These elements of the present paper constitute additional contributions to the difficult and challenging task of elucidating the structure across the scales of complex biophysical signals from the CVS.

5. Conclusion

We studied the peripheral CVS through a multifractal analysis of LDF fluctuations. Our results were compared to ones obtained by the same analysis on HRV fluctuations (central CVS) recorded simultaneously. For this purpose, we first tested four methodologies for the multifractal analysis of our biophysical signals. We compared their applicability and interpretability on synthetic signals possessing known multifractal properties. For this, we selected three multifractal methods (methods from Halsey *et al*, from Chhabra and Jensen, and the structure function method). For each of them, the applicability has been validated against a flexible family of synthetic signals with controllable multifractal properties. At the same time, each of these methods comes with a definition and an implementation which preserve a natural and intuitive interpretation of the results across scales. From these results, these three methods were applied on LDF and HRV fluctuations.

At the biophysical level, our results show that LDF and HRV fluctuations, coming from the peripheral and central CVS, lead to multifractal spectra that are close and rather narrow on the scales studied. These data could therefore present close and weak multifractal properties on these scales. The processed signals come from two different levels of the CVS and are generated by different biophysical mechanisms. It is interesting to note that despite these differences the three multifractal methods used in our study give similar multifractal properties for the signal fluctuations. Moreover, our analysis shows that both kinds of signals present a homogeneous scaling behavior over a range of scales where distinct physiological activities have been reported by authors.

Acknowledgment

Benjamin BUARD acknowledges support from La Région des Pays de la Loire, France.

References

Alam I, Lewis M J, Morgan J and Baxter J 2009 Linear and nonlinear characteristics of heart rate time series in obesity and during weight-reduction surgery *Physiol. Meas.* **30** 541–57

Amaral L A N, Ivanov P Ch, Aoyagi N, Hidaka I, Tomono S, Goldberger A L, Stanley H E and Yamamoto Y 2001 Behavioral-independent features of complex heartbeat dynamics *Phys. Rev. Lett.* **86** 6026–9

Baillie R T, Cecen A A and Erkal C 2009 Normal heartbeat series are nonchaotic, nonlinear, and multifractal: new evidence from semiparametric and parametric tests *Chaos* **19** 028503

Barabasi A L and Vicsek T 1991 Multifractality of self-affine fractals *Phys. Rev.* A **44** 2730–3

Bernjak A, Clarkson P B M, McClintock P V E and Stefanovska A 2008 Low-frequency blood flow oscillations in congestive heart failure and after β1-blockade treatment *Microvasc. Res.* **76** 224–32

Binzoni T, Leung T S and Van De Ville D 2009 The photo-electric current in laser-Doppler flowmetry by Monte Carlo simulations *Phys. Med. Biol.* **54** N303–18

Bracic Lotric M, Stefanovska A, Stajer D and Urbancic-Rovan V 2000 Spectral components of heart rate variability determined by wavelet analysis *Physiol. Meas.* **21** 441–57

Chau N P, Chanudet X, Bauduceau B, Gautier D and Larroque P 1993 Fractal dimension of heart rate and blood pressure in healthy subjects and in diabetic subjects *Blood Press.* **2** 101–7

Chhabra A and Jensen R V 1989 Direct determination of the $f(\alpha)$ singularity spectrum *Phys. Rev. Lett.* **62** 1327–30

Ching E S C and Tsang Y K 2007 Multifractality and scale invariance in human heartbeat dynamics *Phys. Rev.* E **76** 041910

Evertsz C J and Mandelbrot B B 1992 Multifractal measures *Chaos and Fractals. New Frantiers of Science* ed H O Peitgen, H Jürgens and D Saupe (New York: Springer) pp 921–54

Feder J 1988 *Fractals* (New York: Plenum)

Guzman-Vargas L, Munoz-Diosdado A and Angulo-Brown F 2005 Influence of the loss of time-constants repertoire in pathologic heartbeat dynamics *Physica* A **348** 304–16

Halsey T C, Jensen M H, Kadanoff L P, Procaccia I and Shraiman B I 1986 Fractal measures and their singularities *Phys. Rev.* A **33** 1141–51

Havlin S, Amaral L A N, Ashkenazy Y, Goldberger A L, Ivanov P Ch, Peng C K and Stanley H E 1999 Application of statistical physics to heartbeat diagnosis *Physica* A **274** 99–110

Humeau A, Buard B, Chapeau-Blondeau F, Rousseau D, Mahe G and Abraham P 2009 Multifractal analysis of central (electrocardiography) and peripheral (laser Doppler flowmetry) cardiovascular time series from healthy human subjects *Physiol. Meas.* **30** 617–29

Humeau A, Koitka A, Abraham P, Saumet J L and L'Huillier J P 2004 Spectral components of laser Doppler flowmetry signals recorded in healthy and type 1 diabetic subjects at rest and during a local and progressive cutaneous pressure application: scalogram analyses *Phys. Med. Biol.* **49** 3957–70

Humeau A, Steenbergen W, Nilsson H and Strömberg T 2007 Laser Doppler perfusion monitoring and imaging: novel approaches *Med. Biol. Eng. Comput.* **45** 421–35

Ivanov P Ch, Amaral L A N, Goldberger A L, Havlin S, Rosenblum M G, Stanley H E and Struzik Z R 2001 From 1/f noise to multifractal cascades in heartbeat dynamics *Chaos* **11** 641–52

Ivanov P Ch, Amaral L A N, Goldberger A L, Havlin S, Rosenblum M G, Struzik Z R and Stanley H E 1999 Multifractality in human heartbeat dynamics *Nature* **399** 461–5

Kestener P and Arneodo A 2003 Three-dimensional wavelet-based multifractal method: the need for revisiting the multifractal description of turbulence dissipation data *Phys. Rev. Lett.* **91** 194501

Kvandal P, Landsverk S A, Bernjak A, Stefanovska A, Kvernmo H D and Kirkebøen K A 2006 Low-frequency oscillations of the laser Doppler perfusion signal in human skin *Microvasc. Res.* **72** 120–7

Liebert A, Zolek N and Maniewski R 2006 Decomposition of a laser-Doppler spectrum for estimation of speed distribution of particles moving in an optically turbid medium: Monte Carlo validation study *Phys. Med. Biol.* **51** 5737–51

Mandelbrot B B 1999 *Multifractals and 1/F Noise: Wild Self-Affinity in Physics (1963–1976)* (New York: Springer)

Morales F, Graaff R, Smit A J, Bertuglia S, Petoukhova A L, Steenbergen W, Leger P and Rakhorst G 2005 How to assess post-occlusive reactive hyperaemia by means of laser Doppler perfusion monitoring: application of a standardised protocol to patients with peripheral arterial obstructive disease *Microvasc. Res.* **69** 17–23

Munoz-Diosdado A, Guzman-Vargas L, Ramirez-Rojas A, Dek Rio-Correa J L and Angulo-Brown F 2005 Some cases of crossover behavior in heart interbeat and electroseismic time series *Fractals* **13** 253–63

Muzy J F, Bacry E and Arneodo A 1993 Multifractal formalism for fractal signals: the structure-function approach versus the wavelet-transform modulus-maxima method *Phys. Rev.* E **47** 875–84

Popivanov D, Mineva A, Bendayan P, Leger P, Boccalon H and Moller K O 1999 Dynamic characteristics of laser-Doppler flux in normal individuals and patients with Raynaud's phenomenon before and after treatment with nifedipine under different thermal conditions *Technol. Health Care* **7** 193–203

Rajan V, Varghese B, van Leeuwen T G and Steenbergen W 2009 Review of methodological developments in laser Doppler flowmetry *Lasers Med. Sci.* **24** 269–83

Sassi R, Signorini M G and Cerutti S 2009 Multifractality and heart rate variability *Chaos* **19** 028507

Shepherd A P and Öberg P A 1990 *Laser-Doppler Blood Flowmetry* (Dordrecht: Kluwer)
Stanley H E, Amaral L A N, Goldberger A L, Havlin S, Ivanov P Ch and Peng C K 1999 Statistical physics and physiology: monofractal and multifractal approaches *Physica* A **270** 309–24
Stefanovska A, Bracic M and Kvernmo H D 1999 Wavelet analysis of oscillations in the peripheral blood circulation measured by laser Doppler technique *IEEE Trans. Biomed. Eng.* **46** 1230–9
Stern M D 1975 *In vivo* evaluation of microcirculation by coherent light scattering *Nature* **254** 56–8
Turiel A, Perez-Vicente C J and Grazzini J 2006 Numerical methods for the estimation of multifractal singularity spectra on sampled data: a comparative study *J. Comput. Phys.* **216** 362–90
Wojtkiewicz S, Liebert A, Rix H, Zolek N and Maniewski R 2009 Laser-Doppler spectrum decomposition applied for the estimation of speed distribution of particles moving in a multiple scattering medium *Phys. Med. Biol.* **54** 679–97
Yordanova E, Grzesiak M, Wernik A W, Popielawska B and Stasiewicz K 2004 Multifractal structure of turbulence in the magnetospheric cusp *Ann. Geophys.* **22** 2431–40